Charge-Transfer States Determine Iron Porphyrin Film Third-Order Nonlinear Optical Properties in the near-IR Spectral Region

Jonathan Humphrey and Darius Kuciauskas*

Department of Chemistry, Virginia Commonwealth University, 1001 West Main Street, P.O. Box 842006, Richmond, Virginia 23284-2006

Received: April 1, 2004; In Final Form: June 1, 2004

Femtosecond degenerate four-wave mixing (DFWM) was used to study third-order nonlinear optical properties of electropolymerized Fe(III) tetrakis(*p*-hydroxyphenyl)porphyrin films. Third-order nonlinear susceptibility $\chi_{1111}^{(3)}(-\omega;\omega,\omega,-\omega)$ was determined at 760−1350 nm. Susceptibility $\chi^{(3)}$ values for a 500 nm thick porphyrin film ranged between $(2-15)\times10^{-20}$ m^2V^{-2} ($(1.4-10.7)\times10^{-12}$ esu). The time response of electronic nonlinearities was faster than 120 fs. The sum-over-states model was applied to determine real and imaginary components for $\chi^{(3)}$ and molecular second hyperpolarizability, γ. At wavelengths <800 nm, porphyrin film $\chi^{(3)}$ is enhanced due to the 700 nm one-photon charge-transfer (CT) band. Nonlinear properties at longer wavelengths are determined by a two-photon resonance with a 17 400 cm^{-1} state. This state was not observed for other porphyrins and is attributed to a two-photon CT transition. Due to the resonance with the two-photon state, porphyrin Im $\chi^{(3)}$ and two-photon absorption cross-section δ increased about 10 times when compared to values in the long-wavelength limit. Because of the contributions of the two-photon state, real component Re $\chi^{(3)}$ had a negative sign in the near-IR spectral range; Re $\chi^{(3)} \approx -6\times10^{-20}$ m^2V^{-2} at 9000−13 000 cm^{-1}. Results suggest that transition metal CT states can improve third-order nonlinear properties of organic materials.

Introduction

Organic materials are actively explored for third-order nonlinear optical applications such as ultrafast all-optical switching, optical memory, optical power limiting, 3D microfabrication, photodynamic therapy, and fluorescence microscopy. The chemist's goal in this work is to design molecules and materials with high nonlinear coefficients and develop models that can predict these characteristics from the molecular structure.[1,2] The efficiency of processes related to two-photon absorption is described by the imaginary part of the material's third-order nonlinear susceptibility, $\chi^{(3)}$, and molecular second hyperpolarizability, γ. Nonlinear refraction is described by the real part of coefficients $\chi^{(3)}$ and γ.

Recently, third-order nonlinear properties of porphyrins, porphyrin polymers, and porphyrin coordination compounds have been extensively studied.[3−15] This is related, in part, to wide porphyrin use in photomedicine and molecular photonics.[16] Many important questions about porphyrin third-order nonlinear properties remain to be addressed. In this paper, we consider the role of charge-transfer (CT) states in determining transition metal porphyrin third-order nonlinear optical properties. We study Fe(III)Cl tetrakis(*p*-hydroxyphenyl)porphyrin (**1**), because of the importance of iron porphyrin CT states in photochemistry and photobiology. CT states can be described as involving electron transfer from the porphyrin macrocycle to the metal d orbitals.[17]

To learn about electronic states giving rise to nonlinear effects, experiments at different wavelengths are necessary; we carried out such studies at 760−1350 nm, in the near-IR wavelength region important for telecommunications. Two-photon absorption spectra (Im $\chi^{(3)}$ spectra) were already reported for several porphyrins.[14,15,18] In contrast, previous nonresonant DFWM or Z-scan studies that allow determination of both Re $\chi^{(3)}$ and Im $\chi^{(3)}$ components were only carried out at a single wavelength.[4−9,11,12] Thus, this paper appears to be the first report of porphyrin Re $\chi^{(3)}$ and Im $\chi^{(3)}$ spectra in the near-IR.

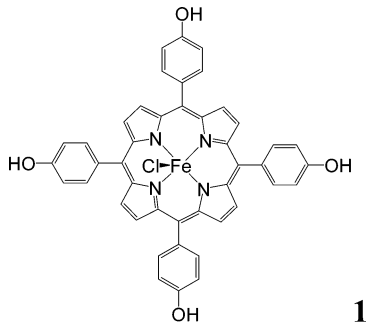

1

We use femtosecond degenerate four-wave mixing (DFWM) to study porphyrin third-order nonlinear spectra. While more complex than other experimental methods, DFWM experiments yield $\chi^{(3)}(-\omega;\omega,\omega,-\omega)$ tensor components important for all-optical information processing applications. DFWM experiments also allow the examination of the time dependence of nonlinear signals.

Both one-photon and two-photon transitions are important for third-order nonlinear effects; therefore, $\chi^{(3)}$ spectra yield properties of two-photon states that cannot be observed using linear spectroscopy. For a molecule with a center of symmetry (D_{4h} symmetry for **1**), a change in parity between the initial and final states is required for an electric dipole allowed one-photon transition. In contrast, two-photon transitions are allowed between states of the same parity. Using quantum chemical

* Corresponding author. E-mail: dkuciauskas@vcu.edu.

10.1021/jp0485643 CCC: $27.50
Published on Web 07/21/2004

SCHEME 1: Schematics of an Optical Setup for Thin Film DFWM Measurements: (A) Arrangement of Laser Beams (1, 2, and 3) and Signal Beam (4, 5, and 6) Propagation Directions; (B) Top and Side Views Showing the Sample, Lens Used for Imaging, Screen, and Photodetector[a]

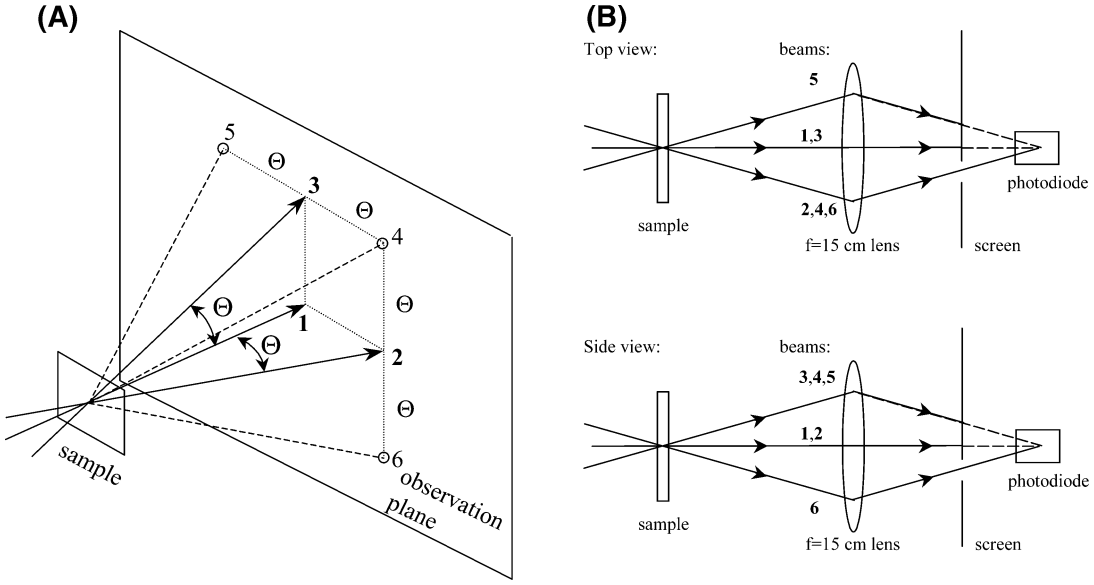

[a] Numbers denote the optical paths of the respective beams.

methods, two-photon $\pi\pi^*$ states for metal-free, Zn(II), and Mg(II) porphyrins were found at 30 000−33 000 cm^{-1}.[19−22] Two-photon fluorescence experiments found metal-free porphyrin two-photon states at similar energies.[13,23] In contrast, we find that much lower energy two-photon states are important for Fe(III) porphyrins. Fe(III) porphyrin film third-order nonlinear susceptibility is enhanced at least several times due to the charge-transfer states.

We investigated porphyrin thin films prepared by electrochemical polymerization.[24−26] Such simple preparation methods afforded films of high optical quality, transparent in near-IR, and stable in air for a long time.

Materials

Fe(III)Cl tetrakis(4-hydroxyphenyl)porphyrin (Porphyrin Systems, Germany), analytical grade organic solvents (Aldrich), and electrochemical grade terabutylammonium perchlorate (TBAP, Fluka) were all used as received. 1737 aluminosilicate glass substrates with and without conductive ITO layer (In_2-[Sn]O_x, resistance 100 Ω) were from Delta Technologies.

Experimental Section

Porphyrin Film Preparation and Characterization. ITO slides were ultrasonically cleansed in demineralized water, 2-propanol, and acetone, dried with a stream of nitrogen, and placed in an oven for a minimum of 15 min prior to film preparation. Porphyrins were dissolved (0.5 mM) in acetonitrile with 0.1 M TBAP as a supporting electrolyte. Nitrogen was bubbled through the solution for 15 min prior to the application of the potential and throughout the film growing process. Porphyrin films on conductive ITO substrates were deposited in cyclic voltammetry and controlled potential experiments; both methods appeared to yield films with the same absorption spectra. For cyclic voltammetry, a conventional three-electrode system consisting of a platinum-working electrode, a platinum wire counter electrode, and an $Ag/AgNO_3$ reference electrode was used. When a two-electrode setup was utilized, a fixed potential (above 500 mV vs ferrocene/ferrocenium) was applied to platinum wire and ITO substrate electrodes. The film was grown for 30 min. The coated substrates were rinsed in acetonitrile and dried with a stream of nitrogen. UV/vis spectra were recorded with an HP-8452A spectrometer. Resonance Raman spectra were acquired with 532 nm excitation (10 mW). SPEX model 1870 0.5 m spectrograph and Princeton Instruments 1340×400 CCD cooled with liquid nitrogen were used. The porphyrin film thickness was determined with a step profilometer. The films were stored in the dark at room temperature; their optical characteristics did not change for several months.

Degenerate Four-Wave Mixing (DFWM). A regeneratively amplified Ti:Sapphire laser system (Spectra Physics) provided 120 fs, 0.8 mJ pulses at 760−840 nm. Experiments at longer wavelength were carried out with excitation from an optical parametric amplifier (OPA TOPAS, Quantronix). Pulses generated by OPA were also 120 fs fwhm; maximal pulse energy (at 1200 nm) was 0.24 mJ. The spectrometer for nonlinear optical experiments was described previously.[27] In DFWM experiments on supported thin film samples, signals have contributions from both the thin film and a thick substrate. As such, it is necessary to separate a thin film optical signal from a substrate signal. As explained below, the optical setup of Scheme 1 allows such separation based on different thin film and thick substrate phase-matching properties.[28]

By using a large (75 mm diameter) $f = 15$ cm lens, we imaged the illuminated sample area to the photodetector (GaInAs photodiode for experiments at $\lambda > 920$ nm, and a PMT for experiments at $\lambda < 920$ nm). A metal screen blocked all beams except the signal beam, which passed through an iris diaphragm. By translating the micrometer-mounted screen, signals **4**, **5**, and **6** could be measured without realigning the optical beams or changing the sample or photodiode position. The time dependence of nonlinear signals was measured by making the optical path of beam **3** longer with a computer-controlled delay line.

In DFWM experiments, three laser beams overlap in the sample as shown in Scheme 1 (angle $\Theta = 4.1°$). When all three laser pulses (**1**, **2**, **3**) reached the sample simultaneously, the signal pulse **4** was generated. Beam **4** propagated in the direction satisfying strict geometric conditions (the phase-matching

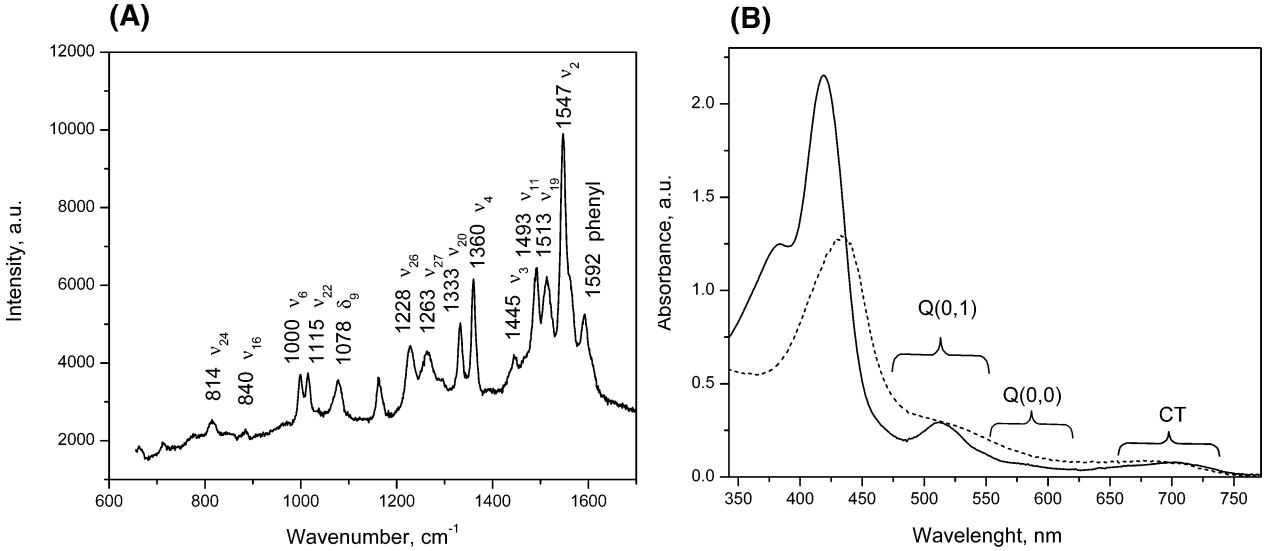

Figure 1. (A) Resonance Raman spectrum of porphyrin film measured with 532 nm excitation. Band assignments are based on variation of band intensities in the polarized Raman spectra.[30] (B) Electronic absorption spectra for **1** in acetonitrile solution (—) and for the porphyrin film (- - -).

conditions can be defined as $\boldsymbol{k}_1 + \boldsymbol{k}_2 = \boldsymbol{k}_3 + \boldsymbol{k}_4$, where $\boldsymbol{k}_i$ are wave vectors of corresponding optical beams *i*). When the sample being investigated consisted of thick substrate and thin film, however, additional signal beams (**5** and **6** in Scheme 1) could be observed.[28] Optical signals **5** and **6** propagate in directions shown in Scheme 1. The power of the phase mismatched signals **5** and **6** was reduced by a factor $F = [\sin(x)/x]^2$, where $x = \Delta kl/2$ and l is the thickness of the medium in which the nonlinear signal is generated.[28] When the angles Θ are small, Δk can be calculated as $\Delta k \approx 2\pi\Theta^2/(n\lambda)$, where n is a refractive index and λ is the wavelength. For a glass substrate, $F = 0.011$ ($l_{\text{glass}} = 0.7$ mm). Therefore, beams **5** and **6** have only negligible contribution from the glass. In contrast, for a thin porphyrin film, $F \approx 1$ ($l_{\text{porphyrin}} = 500$ nm). Therefore, only the thin film nonlinear properties were reflected in non-phase-matched signals **5** and **6**.

All experiments were performed using laser beams of vertical polarization (s-polarization); therefore, the results reflect values of the $\chi_{1111}^{(3)}(-\omega;\omega,\omega,-\omega)$ tensor component. The energy of laser pulses for beams **1**−**3** was 5−15 μJ, and the intensity of the respective beams was 1−10 GW/cm^2. DFWM signals (I_{signal}) had cubic dependence on the excitation intensity, I_{laser}: $I_{\text{signal}} \propto I_{\text{laser}}^{3\pm0.1}$.

Results

Preparation, Absorption Spectra, and Electrochemical Properties of Porphyrin Films. In acetonitrile solution, the Fe(II)/Fe(III) redox couple was reversible; the potential was 620 mV vs ferrocene/ferrocenium. The oxidation and reduction peaks were unchanged in the initial scan when an ITO slide was used as the working electrode. With repetitive scanning, both reduction and oxidation peaks shifted to higher potentials (see cyclic voltammetry data shown in the Supporting Information). The oxidation and reduction waves also increased in amplitude with each scan. Such characteristics indicate that a conductive porphyrin polymer film was growing on the ITO electrode.[25,26] The polymerized film was not soluble in acetonitrile. Porphyrin film properties were investigated with resonance Raman and UV−vis absorption spectroscopy. Resonance Raman data (Figure 1A) allow the determination of the porphyrin oxidation and spin state. As is typical for porphyrins, the bands at 600−1600 cm^{-1} correspond to in-plane porphyrin skeletal modes.[29−31] In particular, frequencies of ν_4 (1360 cm^{-1}, polarized), ν_{19} (1513 cm^{-1}, anomalously polarized), and ν_2 (1547 cm^{-1}, polarized) bands in Figure 1A are characteristic of high-spin, oxidation state III tetraphenyl porphyrins.[29] Therefore, electrochemical polymerization and film formation does not change the porphyrin spin or oxidation state. This result is consistent with the mechanism proposed in the literature: tetrakis(*p*-hydroxyphenyl)porphyrin polymerization occurs by forming bonds between the hydroxyphenyl substituents, while the porphyrin macrocycle and metal remain unaffected.[26]

In agreement with assignment from the Raman spectrum, the electronic absorption spectrum of porphyrin **1** in acetonitrile solution (Figure 1B) is typical of high-spin Fe(III) porphyrins.[32,33] While the intense Soret band and less intense Q-bands characteristic of all porphyrins are present, low energy CT transitions ($a_{1u}(\pi)$, $a_{2u}(\pi) \rightarrow e_g(d_{yz}, d_{zx})$) result in the addition of two peaks at 660 and 700 nm. In comparison to other tetraphenyl Fe(III)Cl porphyrins,[32] hydroxyl groups induce a red shift of CT bands. In addition, the oscillator strength of the purely electronic Q(0,0) band is reduced in comparison to Fe(III)Cl tetraphenyl porphyrin, and this Q(0,0) band is almost completely obscured by a shoulder of the nearby Q(0,1) band. A similar reduction in Q(0,0) band intensity was observed for Fe(III)Cl tetrakis(*p*-metoxyphenyl)porphyrins,[32] which suggests that electron-donating substituents on the phenyl rings reduce Q(0,0) band intensity.

Changes in the film spectrum are consistent with observations of similar systems.[25] The Soret band is red-shifted by approximately 20 nm and considerably broadened, while the Q(0,1) band broadening is significant enough to completely obscure the Q(0,0) band. The CT bands show a slight shift to the blue. Additionally, the Soret band intensity is reduced, and the CT band intensities have increased. The red shift and weakening of Soret band could be attributed to excitonic coupling between adjacent porphyrin molecules. The degree of dipole−dipole interaction is largely a function of transition dipole moment. As the transition dipoles of the Q-bands are approximately 20 times smaller than that of the Soret band, the energies of these transitions are largely unchanged in the film spectrum. The significant band broadening observed in the film spectrum can also be a consequence of inhomogeneity associated with irregular orientations of neighboring molecules.

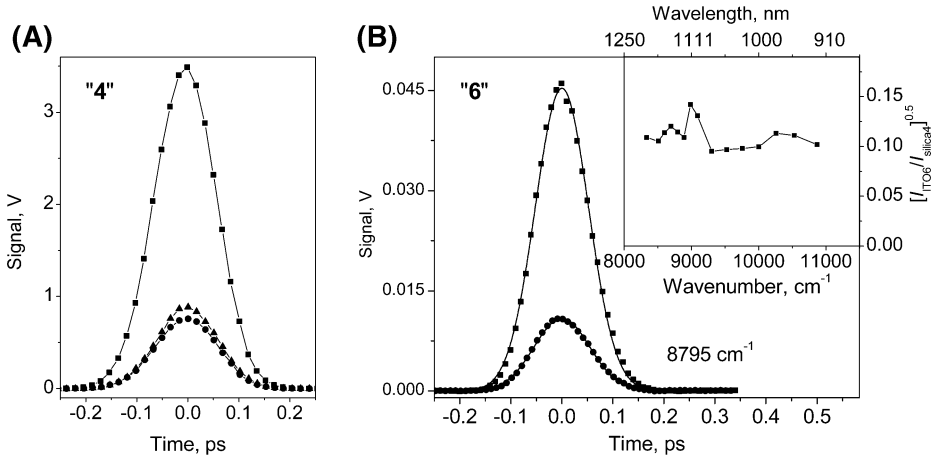

Figure 2. DFWM kinetics measured at 1137 nm (8795 cm^{-1}). (A) Signals measured at position "4" (Scheme 1) for silica reference (■), glass substrate (●), and ITO/glass (▲). (B) Signals measured at position "6" for glass substrate (●) and ITO/glass (■). Inset: ITO film nonlinear spectrum calculated from measurements at the "6" position.

Third-Order Nonlinear Properties of an ITO Substrate. Porphyrin film was electropolymerized on a glass substrate coated with an ITO layer; therefore, we first examine glass and ITO nonlinear properties. Figure 2A shows DFWM kinetics for a silica reference and glass substrates with and without ITO measured at the "4" position (Scheme 1). Silica is a convenient reference material for measurements with femtosecond pulses because its third-order nonlinear susceptibility $\chi_{silica}^{(3)} = 2.04\times10^{-22}$ m^2V^{-2} is independent of wavelength and laser pulse width.[34] ($\chi^{(3)}$ values in SI units can be converted to esu units using the following expression: $\chi^{(3)}(esu) = c^2(4\pi\times10^8)^{-1}\chi^{(3)}(SI)$, where c is the speed of light. Therefore, $\chi_{silica}^{(3)} = 1.46\times10^{-14}$ esu.) The unknown third-order nonlinear susceptibility for glass, $\chi_{glass}^{(3)}$, is obtained from the amplitudes of the DFWM signals, $I_{silica4}$ and I_{glass4}, by using the following equation (correct in the case of a nonabsorbing sample):[35]

$$|\chi_{glass}^{(3)}| = |\chi_{silica}^{(3)}|\sqrt{\frac{I_{glass4}}{I_{silica4}}}\frac{l_{silica}}{l_{glass}}\frac{n_{glass}^2}{n_{silica}^2} \qquad (1)$$

where $l_{silica} = 1.0$ mm and $l_{glass} = 0.7$ mm are the optical path lengths in the two media, and $n_{silica} = 1.46$ and $n_{glass} = 1.53$ are the linear refractive indices. Calculation yields $|\chi_{glass}^{(3)}| = 1.5\times10^{-22}$ m^2V^{-2} (1.1×10^{-14} esu). $\chi_{silica}^{(3)}$ is usually assumed to be real and positive because near-IR wavelengths are very far from one-, two-, and three-photon resonances for this material. Electronic states for glass are at energies similar to those for silica; therefore, we assume that $\chi_{glass}^{(3)}$ also has only a real and positive component, Re $\chi_{glass}^{(3)} \approx |\chi_{glass}^{(3)}| = 1.5\times10^{-22}$ m^2V^{-2}.

Next, we analyze the ITO nonlinear properties. The ITO signal **4** amplitude is very similar to glass signal **4** amplitude (Figure 2A), and determination of ITO nonlinear properties from measurement at position "4" is difficult. As was described in the Experimental Section, it is convenient to determine thin film nonlinear susceptibility $\chi_{ITO}^{(3)}$ from the non-phase-matched signal I_{ITO6} (measured at position "6", Scheme 1). As is evident from Figure 2B, ITO signal **6** is significantly larger than the glass substrate signal. To calculate $\chi_{ITO}^{(3)}$ according to a formula similar to eq 1, we would need to know the thickness of the ITO layer. Our several attempts to measure this thickness were not successful; therefore, we only report $(I_{ITO6}/I_{silica4})^{0.5} = 0.11$ at 1137 nm. The ratio of susceptibilities is then $|\chi^{(3)}|_{ITO}/|\chi^{(3)}|_{silica} = (I_{ITO6}^{0.5}l_{silica}n_{ITO}^2)/(I_{silica4}^{0.5}l_{ITO}n_{silica}^2) = 0.21l_{silica}/l_{ITO}$. The inset in Figure 2B shows the $(I_{ITO6}/I_{silica6})^{0.5}$ spectrum at 920−1210 nm; this ratio is approximately constant. On the basis of this result, we assume that the $\chi_{ITO}^{(3)}$ value does not change in the wavelength range of the study. From the analysis of the porphyrin film $\chi_{film}^{(3)}$ spectrum, the $\chi_{ITO}^{(3)}$ value was estimated as -2×10^{-20} m^2V^{-2} (see Discussion).

Porphyrin Film Third-Order Nonlinear Properties. DFWM kinetics at 1137 nm measured for porphyrin film electropolymerized on glass/ITO substrate are shown in Figure 3A. Both porphyrin and ITO thin films contribute to this non-phase-matched signal, but analysis developed in the Discussion allows the separation of these contributions. In particular, the presence of porphyrin film reduces the 1137 nm signal as compared to ITO/glass substrate (Figure 2B). This reduction is observed because of the interference between the ITO and porphyrin nonlinear signals (a similar effect was reported for thermally evaporated fullerene C_{60} films on CaF_2 substrates).[28] The calculation for the $\chi_{film}^{(3)}$ is based on a formula similar to eq 1, but the porphyrin film signal, $I_{porphyrin6}$, is compared to the silica reference signal, $I_{silica4}$:

$$|\chi_{film}^{(3)}| = |\chi_{silica}^{(3)}|\sqrt{\frac{I_{porphyrin6}}{I_{silica4}}}\frac{l_{silica}}{l_{porphyrin}}\frac{n_{porphyrin}^2}{n_{silica}^2} \qquad (2)$$

Because $n_{porphyrin} = 2.0$[9] and $l_{porphyrin} = 500$ nm, $\chi_{film}^{(3)} = 8.0\times10^{-20}$ m^2V^{-2} (5.7×10^{-12} esu) at 1137 nm.

In addition to amplitudes, it is important to consider the time dependence of the DFWM signals. If excited states are formed following irradiation, much can be learned about the properties of the excited states and intermolecular interactions from the excited-state and the ground-state kinetics. On the other hand, for some nonlinear optical applications, it is desirable to avoid formation of excited states, as absorption leads to attenuation of optical beams and can induce photochemical damage to the material. As is evident from Figure 3A (also Figure 2A and B), all kinetics have fwhm≈125 fs, which is equal to the autocorrelation function width of the laser pulse. Porphyrin film DFWM kinetics in Figure 3A decay to <1% of the initial amplitude in about 200 fs, which suggests that nonlinearities are purely electronic and nonresonant. Different results were obtained for Zn(II) porphyrin polymer films in experiments with picosecond pulses at 1064 nm, where residual amplitudes were significant.[9] Use of lower energy (but higher peak power) femtosecond pulses in our experiments allows better characterization of porphyrin polymer films by eliminating resonant and thermal effects.

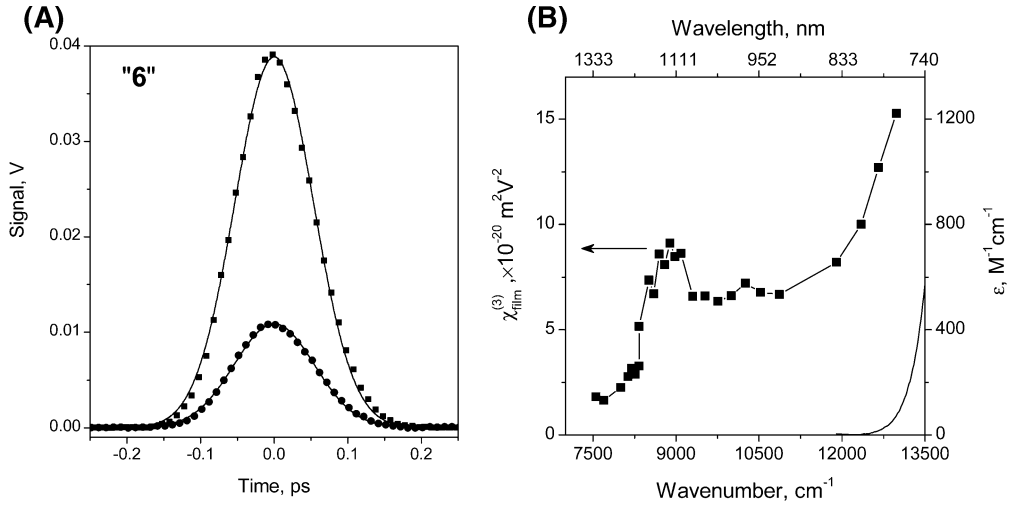

Figure 3. (A) 1137 nm DFWM kinetics measured at the "6" position for porphyrin film (■), and for glass substrate (●). (B) Third-order nonlinear susceptibility spectrum (■) at 760−1350 nm. For comparison, the linear absorption spectrum (—) for porphyrin film is also shown.

Similar experiments measuring nonlinear signals at the "4" and "6" positions were carried out at other wavelengths between 760 and 1350 nm. Figure 3B shows the $\chi_{film}^{(3)}$ spectrum obtained from measurements taken at position "6". Because the ITO substrate signal amplitude is approximately constant in this wavelength range (inset in Figure 2B), spectral features are due to Fe(III)Cl porphyrin film. The peak at ∼8700 cm^{-1} (∼1150 nm) is in the wavelength region with no one-photon absorption (one-photon absorption spectrum is also shown in Figure 3B), but the 8700 cm^{-1} peak can be related to two-photon processes. Analysis developed in the Discussion allows the determination of porphyrin real and imaginary second hyperpolarizability values and confirms the 8700 cm^{-1} peak assignment to the two-photon absorption process.

Nonlinear optical effects higher than third-order (such as three-photon absorption) have been observed for organic molecules at high excitation intensities,[36] but we conclude that higher-order processes do not contribute significantly to the nonlinear spectrum in Figure 3B. DFWM signals had cubic dependence on the excitation intensity, which is characteristic of the $\chi^{(3)}$ process. Higher-order processes (for example, three-photon absorption is described by $\chi^{(5)}$ nonlinear susceptibility) should have different intensity dependence in DFWM experiments. In addition, absorption to the Soret band with the maximum at 436 nm (22 936 cm^{-1}, Figure 1B) cannot be achieved with three 8700 cm^{-1} photons. Because the selection rules for one- and three-photon transitions are the same, three-photon transition energies usually match linear absorption peaks well.[37] Therefore, we do not consider higher-order processes when analyzing the spectrum in Figure 3B.

Next, we consider the increase in $\chi_{film}^{(3)}$ values at >11 000 cm^{-1} in Figure 3B. The porphyrin CT absorption band has a maximum at 14 300 cm^{-1} and fwhm of 1020 cm^{-1}, and some absorption can be observed down to 12 500 cm^{-1}. Therefore, larger $\chi_{film}^{(3)}$ values in this spectral region can be related to the resonance enhancement. Rebane and co-workers have found that metal-free porphyrin two-photon absorption at ∼12 500 cm^{-1} is enhanced due to: (1) near-resonance with the longest wavelength absorption band (Q(0,0) band in the case of metal-free porphyrins), and (2) two-photon (g symmetry) states at ∼26 000 cm^{-1}.[13] Similar energy two-photon states for metal-free porphyrins were also predicted in calculations.[19−22] We cannot rule out that $\chi_{film}^{(3)}$ at >11 000 cm^{-1} has contributions from similar two-photon states; however, modeling shows that $\chi_{film}^{(3)}$ values in this spectral region can be well-approximated by only resonant contribution.

Discussion

Porphyrin Interactions in Electropolymerized Film. Electrosynthesis was previously used to prepare porphyrin films for electrochemical and optical studies.[24−26] Murray and co-workers proposed that the formation of hydroxyphenyl porphyrin films is analogous to the electropolymerization of phenol.[25] Starting from this assumption, Savenije et al. have investigated the mechanism of Zn(II) tetrakis(*p*-hydroxyphenyl)porphyrin film formation and proposed that an ether bond forms between adjacent porphyrins at the meta carbon of the phenyl ring.[26] These workers also determined that the porphyrin macrocycle is not affected by the polymerization process. Our studies support this conclusion. The porphyrin film does not dissolve in acetonitrile, whereas porphyrin monomers are highly soluble in this solvent. From resonance Raman and electronic absorption spectra (Figure 1), we find that iron porphyrin oxidation and spin states do not change during polymerization. Absorption bands broaden and shift significantly, indicating electronic interactions between the porphyrins; however, Raman and UV−vis data indicate that the porphyrin macrocycle is not affected by polymerization. While the porphyrins are linked by covalent bonds, DFWM data indicate that electronic coupling between adjacent porphyrins is not strong. It is well-known that phenyl groups substituted at porphyrin meso-positions form a dihedral angle with the porphyrin plane (∼60° in solution).[38] This geometry reduces electronic coupling between porphyrins connected through meta phenyl linkages. The increase in electronic coupling is expected to yield large hyperpolarizability values,[7,9,11,12,15] and electropolymerization of porphyrins with different linkers that do not include the phenyl groups may yield films with higher nonlinear susceptibilities.[24] Current films provide an opportunity to investigate effects due to Fe(III) CT states.

Real and Imaginary Components of the Third-Order Nonlinear Susceptibility Tensor. The goal in this section is to separate porphyrin two-photon absorption (Im $\chi^{(3)}$) and nonlinear refraction (Re $\chi^{(3)}$) contributions to the spectrum shown in Figure 3B. We also take into account Re $\chi^{(3)}$ for the ITO layer. We start by using a sum-over-states description for the molecular second hyperpolarizability.[2,39] We simplify general sum-over-states model by assuming that three states (ground state, one-photon and two-photon states) are required to describe

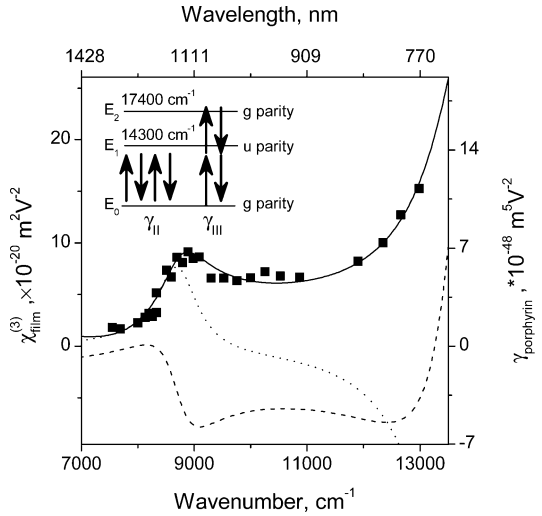

Figure 4. Real (- - -) and imaginary (····) components of the third-order nonlinear susceptibility (■) of Fe(III) porphyrin film. The right axis shows the corresponding porphyrin molecular hyperpolarizability values. Inset: Energy levels used in the simulation. Arrows illustrate γ_{II} and γ_{III} processes contributing to the third-order nonlinearity (see eq 3).

the porphyrin second hyperpolarizability, $\gamma_{porphyrin}$. In this case, $\gamma_{porphyrin}$ is expressed as the sum of three terms, γ_I, γ_{II}, and γ_{III}:

$$\gamma_{porphyrin} \propto \frac{M_{01}^2 \Delta\mu^2}{(\omega_1 - \omega - i\Gamma_1)^3} - \frac{M_{01}^4}{(\omega_1 - \omega - i\Gamma_1)^3} + \frac{M_{01}^2 M_{12}^2}{(\omega_1 - \omega - i\Gamma_1)^2(\omega_2 - 2\omega - i\Gamma_2)} = \gamma_I + \gamma_{II} + \gamma_{III} \quad (3)$$

where $\Delta\mu = \mu_{11} - \mu_{00}$ is the dipole moment difference between the first excited and the ground state, M_{01} and M_{12} are the transition dipole moments for the $0 \rightarrow 1$ and $1 \rightarrow 2$ transitions, ω is the frequency used in the experiment, ω_1 and ω_2 are the frequencies derived from the excited-state energies E_1 and E_2 ($\omega_1 = E_1/\hbar$ and $\omega_2 = E_2/\hbar$; $\hbar$ is reduced Planck's constant), and Γ_1 and Γ_2 are dephasing parameters that account for the linewidths. Porphyrin dipole moments in the ground and excited states are similar (typical porphyrin Stokes shifts are only several nanometers), and $\Delta\mu$ is much smaller than M_{01} and M_{12}. Therefore, in the first approximation, γ_I can be neglected in the analysis and only γ_{II} and γ_{III} terms will be considered. Term γ_{II} describes resonant one-photon contribution to third-order nonlinearity, and γ_{III} describes two-photon processes (see inset in Figure 4). M_{01} can be obtained by integrating the porphyrin absorption spectrum in the CT band region:

$$M_{01} = \frac{1500(\hbar c)^2 \ln 10}{\pi N_A E_1} \int \epsilon(\nu)\, d\nu \quad (4)$$

where N_A is Avogadro's number, $\epsilon(\nu)$ is the extinction coefficient, c is the speed of light, and ν is the wavenumber. Calculation yields $M_{01} = 1.3$ D (4.3×10^{-29} C m in SI units). M_{12} describes the transition between the excited one-photon state and a two-photon state and could be estimated using a formula similar to eq 4 if excited-state extinction coefficients were known. In the visible spectral range, porphyrin excited-state extinction coefficients have values similar to the ground-state extinction coefficients.[18,40] We are not aware of Fe(III) porphyrin excited-state extinction coefficient measurements at 1000−1500 nm and will treat M_{12} as an adjustable parameter. The second unknown parameter in eq 3 is the energy of the two-photon state, E_2. $E_1 = 14\,300$ cm^{-1} corresponds to the CT band in the linear absorption spectrum. For Γ_1 and Γ_2, we use 900 cm^{-1}, similar to the width of the CT absorption band. A bandwidth of this order corresponds to the electronic dephasing time of 10 fs ($T_2 = \hbar/\Gamma_{01}$), typical of porphyrins.[41]

Assuming random porphyrin orientation in the electropolymerized film, porphyrin film nonlinear susceptibility $\chi_{porphyrin}^{(3)}$ is related to the molecular hyperpolarizability $\gamma_{porphyrin}$ as:

$$\chi_{porphyrin}^{(3)} = Nf^4\gamma_{porphyrin} \quad (5)$$

where f is the local field factor, $f = (n^2 + 2)/3$; $f = 2.0$ based on $n = 2.0$ (refractive index was determined for a spin-cast porphyrin polymer film[9]). From Beer's law, the molecular number density $N = 1000AN_A/(\epsilon l_{porphyrin})$, where A is the absorption at the maximum of the Q(0,1) band. $N = 6.2\times10^{26}$ molecules m^{-3} based on $A = 0.64$ and $\epsilon = 1.25\times10^4$ M^{-1} cm^{-1} at 700 nm. Finally, the total nonlinear susceptibility $\chi_{film}^{(3)}$ is:

$$\chi_{film}^{(3)} = \mathrm{Re}(Nf^4\gamma_{poprhyrin} + \chi_{ITO}^{(3)}) + iNf^4\mathrm{Im}(\gamma_{porphyrin}) \quad (6)$$

Equations 3 and 6 were used to simulate the experimental $\chi_{film}^{(3)}$ spectrum; Figure 4 shows the results, real, imaginary, and absolute values of the third-order nonlinear susceptibility and molecular hyperpolarizability. The determined transition dipole moment $M_{12} = 4.2$ D has a value similar to that of M_{01}. The excited two-photon state energy determined in simulation is $E_2 = 17\,400$ cm^{-1}. The presence of such a state is evident in the spectrum, and variation of other fitting parameters does not change the E_2 value. Re $\chi_{ITO}^{(3)}$ determined in simulation is -2×10^{-20} m^{2}V^{-2}. Next, we analyze Re $\chi_{film}^{(3)}$ and Im $\chi_{film}^{(3)}$ spectra from Figure 4.

Two-Photon Absorption in Fe(III) Porphyrin Film. From the Im $\gamma_{porphyrin}$ value, we calculate the two-photon absorption cross section, δ, which is commonly used to report two-photon absorption efficiency (ϵ_0 is the electric constant):[2]

$$\delta(\omega) = \frac{6\pi^2\hbar}{\epsilon_0 n^2 \lambda^2} f^4 \mathrm{Im}\gamma(-\omega;\omega,\omega,-\omega) \quad (7)$$

One-photon and two-photon absorption spectra are compared in Figure 5. The frequency axis of the two-photon spectrum (top axis) is divided by 2, because the energies of the two photons are added in a two-photon transition. Such a graph can be used to evaluate two-photon absorption when laser frequency is tuned between 6000 and 11 000 cm^{-1} (1660−900 nm). When shown in this way, the two-photon absorption band overlaps the weak Q(0,0) band in the one-photon spectrum (also see Figure 1).

We first consider if the two-photon absorption is enhanced due to overlap with the Q(0,0) band. Metal porphyrins have D_{4h} symmetry, and therefore porphyrin electronic ground state has g parity. One-photon absorption corresponds to an allowed electronic transition from a g parity ground state to a u parity excited state. Selection rules for two-photon transitions are opposite: two-photon absorption is allowed for an electronic transition from the g parity ground state to the same, g, parity excited state. Therefore, for a porphyrin with D_{4h} symmetry, two-photon absorption to a Q(0,0) band is not allowed. However, phenyl rotation or intramolecular interactions can reduce porphyrin symmetry and make two-photon absorption in the Q-band region possible. Kruk et al. have proposed that this effect is more significant for the Q(0,1) band because the

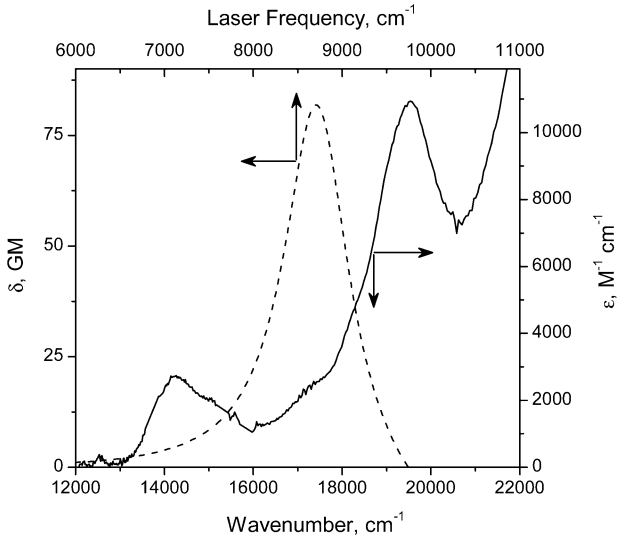

Figure 5. Linear absorption spectrum (—) and two-photon absorption spectrum (- - -) for Fe(III) porphyrin film (GM units were used for δ; 1 GM = 1×10^{-50} cm^{4}s).

Q(0,1) band has both electronic and vibrational contributions and reduction in symmetry changes the parity of vibrational wave functions.[23] We observe the opposite case − two-photon absorption is stronger in the purely electronic Q(0,0) band region but not in the vibrational/electronic Q(0,1) band region. Therefore, changes in symmetry are not likely to lead to two-photon absorption to the Q(0,1) band, and a different origin of two-photon absorption should be considered.

Next, we consider if porphyrin macrocycle $\pi\pi^*$ two-photon states could explain the two-photon spectrum in Figure 5. Two-photon states for several (but not iron) porphyrins have been investigated at different levels of theory.[19−22] Metal-free,[19,21] Zn(II),[22] and Mg(II)[20] porphyrin two-photon states were found at 30 000−33 000 cm^{-1} in the Soret, but not the Q-band region. Electronic interaction between porphyrins can lower the energies of the two-photon states, but such interactions also lead to significant changes in the one-photon spectrum.[22] The porphyrin **1** film one-photon spectrum is similar to the **1** spectrum in solution (Figure 1); therefore, it is unlikely that the energy of $\pi\pi^*$ two-photon states could change from ∼30 000 to 17 400 cm^{-1}.

Because the iron porphyrin **1** two-photon spectrum is different from a metal-free porphyrin two-photon spectrum (as well from spectra of other metal-free tetrapyrrolic compounds)[14] and Q(0,0) band overlap or $\pi\pi^*$ two-photon states cannot explain this difference, we speculate that the 17 400 cm^{-1} state is likely to be an Fe(III) CT state. It would be interesting to examine such an assignment in calculations. An alternative explanation would involve intermolecular charge transfer and excimer formation.

Karotki et al. have measured $\delta = 1-6$ GM for a metal-free tetraphenyl porphyrin in the 1100−1400 nm range.[14] In the zero-frequency (low energy) limit, a similar δ value can be extrapolated for **1** (Figures 4 and 5). In the near-IR wavelength range, δ for **1** is significantly higher (δ_{max} = 82 GM at 1150 nm), which is attributed to a two-photon resonance due to CT states. Several molecular design strategies could be used to further increase the porphyrin two-photon absorption cross section. Such approaches include substitution with donor/acceptor groups for porphyrins,[13] porphyrin self-assembly,[15] as well as the more general use of donor and acceptor motifs.[42,43] Data for iron porphyrin **1** demonstrate that transition metal two-photon states can also be important in optimizing δ values in organic materials.

Nonlinear Refraction in Fe(III) Porphyrin Film. Nonlinear susceptibility Re $\chi^{(3)}(-\omega;\omega,\omega,-\omega)$ measured in the DFWM experiment is directly related to optical switching and other effects based on nonlinear changes in the index of refraction.[2] This paper appears to be the first report of the porphyrin Re $\chi^{(3)}(-\omega;\omega,\omega,-\omega)$ spectrum in the near-IR spectral region. Previous nonresonant studies were carried out at a single wavelength of 1064[6,7,9,11] or ∼800 nm.[8,10,12]

As shown in Figure 4, Fe(III) porphyrin film has a negative Re $\chi^{(3)}_{film}$ in a broad spectral range. The value for molecular hyperpolarizability is Re $\gamma_{porphyrin} \approx -5\times10^{-48}$ m^{5}V^{-2} at 9000−13 000 cm^{-1}. According to eq 3, Re $\gamma_{porphyrin}$ is negative when the photon energy is higher than $E_2/2$ ($2\hbar\omega > E_2$). Organic nonlinear materials with Re $\chi^{(3)} < 0$ are not common,[44] but are potentially important, because in such materials laser light is defocused, thus protecting the material from optical damage (in contrast, materials with positive Re $\chi^{(3)}$ focus light).

Metal-free and Zn(II) porphyrins also have negative Re γ values at 1064[6,7] and 800 nm;[8] contributions from two-photon states were used to explain this sign. Because two-photon spectra for metal-free porphyrins are different from Fe(III) porphyrins (see previous section), different two-photon states must be relevant for metal-free and Zn(II) porphyrin $\chi^{(3)}$ frequency dispersion in the near-IR spectral range. Detailed studies of other organic materials have shown that more than three states could be required to explain $\chi^{(3)}$ frequency dispersion.[45] Measurements of $\chi^{(3)}$ spectra for other porphyrins would show if this is the case for tetrapyrrolic compounds.

Conclusions

We report detailed femtosecond DFWM studies of Fe(III) porphyrin electropolymerized films and find that $\chi_{film}^{(3)}$ and $\gamma_{porphyrin}$ frequency dependence in near-IR are well described by a three-level model. An increase in nonlinear coefficients at ∼800 nm is due to the near-resonance enhancement in the CT band; these characteristics are similar to those of other porphyrins. In addition, a two-photon state at 17 400 cm^{-1} was identified. Such states were previously not observed for metal-free tetrapyrrolic compounds; therefore, it is attributed to CT transitions. Due to the resonance with the two-photon state, $\chi_{film}^{(3)}$ increased more than 10 times when compared to values in the long-wavelength limit. The time response of nonresonant electronic third-order nonlinearity in porphyrin films is faster than 120 fs.

Acknowledgment. We thank Dr. James Terner for resonance Raman measurements and spectral assignments, Dr. Michael A. Reshchikov for porphyrin film thickness measurements, and Dr. Fred M. Hawkridge for help with electrochemistry experiments. D.K. acknowledges support from VCU.

Supporting Information Available: Figures S1 and S2 showing the cyclic voltammograms for Fe(III)Cl tetrakis(*p*-hydroxyphenyl)porphyrin measured with Pt and ITO working electrodes. This material is available free of charge via the Internet at http://pubs.acs.org.

References and Notes

(1) Tykwinski, R. R.; Gubler, U.; Martin, R. E.; Diederich, F.; Bosshard, C.; Gunter, P. *J. Phys. Chem. B* **1998**, *102*, 4451.

(2) Gubler, U.; Bosshard, C. In *Polymers in Photonics Applications I*; Lee, K.-S., Ed.; Springer: Berlin, 2002; p 123.

(3) Blau, W.; Byrne, H.; Dennis, W. M.; Kelly, J. M. *Opt. Commun.* **1985**, *56*, 25.
(4) Guha, S.; Kang, K.; Porter, P.; Roach, J. F.; Remy, D. E.; Aranda, F. J.; Rao, D. V. G. L. N. *Opt. Lett.* **1992**, *17*, 264.
(5) Fei, H.; Han, L.; Ai, X.; Yin, R.; Shen, J. *Chin. Sci. Bull.* **1992**, *37*, 298.
(6) Terazima, M.; Shimizu, H.; Osuka, A. J. *Appl. Phys.* **1997**, *81*, 2946.
(7) Thorne, J. R. G.; Kuebler, S. M.; Denning, R. G.; Blake, I. M.; Taylor, P. N.; Anderson, H. L. *Chem. Phys.* **1999**, *248*, 181.
(8) Kandasamy, K.; Shetty, S. J.; Puntambekar, P. N.; Srivastava, T. S.; Kundu, T.; Singh, B. P. *J. Porphyrins Phthalocyanines* **1999**, *3*, 81.
(9) Kuebler, S. M.; Denning, R. G.; Anderson, H. L. *J. Am. Chem. Soc.* **2000**, *122*, 339.
(10) Kano, H.; Kobayashi, T. *Opt. Commun.* **2000**, *178*, 133.
(11) Screen, T. E. O.; Thorne, J. R. G.; Denning, R. G.; Bucknell, D. G.; Anderson, H. L. *J. Am. Chem. Soc.* **2002**, *124*, 9712.
(12) Ogawa, K.; Zhang, T. Q.; Yoshihara, K.; Kobuke, Y. *J. Am. Chem. Soc.* **2002**, *124*, 22.
(13) Drobizhev, M.; Karotki, A.; Kruk, M.; Mamardashvili, N. Z.; Rebane, A. *Chem. Phys. Lett.* **2002**, *361*, 504.
(14) Karotki, A.; Drobizhev, M.; Kruk, M.; Spangler, C.; Nickel, E.; Mamardashvili, N.; Rebane, A. *J. Opt. Soc. Am. B-Opt. Phys.* **2003**, *20*, 321.
(15) Ogawa, K.; Ohashi, A.; Kobuke, Y.; Kamada, K.; Ohta, K. *J. Am. Chem. Soc.* **2003**, *125*, 13356.
(16) Prasad, P. N. *Introduction to Biophotonics*; Wiley: New York, 2003.
(17) Gouterman, M. *J. Chem. Phys.* **1959**, *30*, 1139.
(18) Drobizhev, M.; Karotki, A.; Kruk, M.; Rebane, A. *Chem. Phys. Lett.* **2002**, *355*, 175.
(19) Masthay, M. B.; Findsen, L. A.; Pierce, B. M.; Bocian, D. F.; Lindsey, J. S.; Birge, R. R. *J. Chem. Phys.* **1985**, *84*, 3901.
(20) Kuzmitsky, V. A. *J. Appl. Spectrosc.* **2001**, *68*, 758.
(21) Liu, X. J.; Feng, J. K.; Ren, A. M.; Zhou, X. *Chem. Phys. Lett.* **2003**, *373*, 197.
(22) Zhou, X.; Ren, A. M.; Feng, J. K.; Liu, X. J.; Zhang, Y. D. *ChemPhysChem* **2003**, *4*, 991.
(23) Kruk, M.; Karotki, A.; Drobizhev, M.; Kuzmitsky, V.; Gael, V.; Rebane, A. *J. Lumin.* **2003**, *105*, 45.
(24) Bedioui, F.; Devynck, J.; Bied-Charreton, C. *Acc. Chem. Res.* **1995**, *28*, 30.
(25) Bettelheim, A.; White, B. A.; Raybuck, S. A.; Murray, R. W. *Inorg. Chem.* **1987**, *26*, 1009.
(26) Savenije, T. J.; Koehorst, R. B. M.; Schaafsma, T. J. *J. Phys. Chem. B* **1997**, *101*, 720.
(27) Kuciauskas, D.; Porsch, M. J.; Pakalnis, S.; Lott, K. M.; Wright, M. E. *J. Phys. Chem. B* **2003**, *107*, 1559.
(28) Strohkendl, F. P.; Dalton, L. R.; Hellwarth, R. W.; Sarkas, H. W.; Kafafi, Z. H. *J. Opt. Soc. Am. B-Opt. Phys.* **1997**, *14*, 92.
(29) Oshio, H.; Ama, T.; Watanabe, T.; Kincaid, J.; Nakamoto, K. *Spectrochim. Acta* **1984**, *40A*, 863.
(30) Li, X. Y.; Czernuszewicz, R. S.; Kincaid, J. R.; Su, Y. O.; Spiro, T. G. *J. Phys. Chem.* **1990**, *94*, 31.
(31) Jayaraj, K.; Terner, J.; Gold, A.; Roberts, D. A.; Austin, R. N.; Mandon, D.; Weiss, R.; Bill, E.; Muther, M.; Trautwein, A. X. *Inorg. Chem.* **1996**, *35*, 1632.
(32) Ohya, T.; Sato, M. *Bull. Chem. Soc. Jpn.* **1996**, *69*, 3201.
(33) Kobayashi, H.; Yanagawa, Y.; Osada, H.; Minami, S.; Shimizu, M. *Bull. Chem. Soc. Jpn.* **1973**, *46*, 1471.
(34) Milam, D. *Appl. Opt.* **1998**, *37*, 546.
(35) Prasad, P. N.; Williams, D. J. *Introduction to Nonlinear Optical Effects in Molecules and Polymers*; John Willey & Sons: New York, 1991.
(36) He, G. S.; Markowicz, P. P.; Lin, T. C.; Prasad, P. N. *Nature* **2002**, *415*, 767.
(37) Drobizhev, M.; Karotki, A.; Kruk, M.; Dzenis, Y.; Rebane, A.; Suo, Z.; Spangler, C. W. *J. Phys. Chem. B* **2004**, *108*, 4221.
(38) Gust, D.; Moore, T. A.; Moore, A. L.; Devadoss, C.; Liddell, P. A.; Hermant, R.; Nieman, R. A.; Demanche, L. J.; DeGraziano, J. M.; Gouni, I. *J. Am. Chem. Soc.* **1992**, *114*, 3590.
(39) Orr, B. J.; Ward, J. F. *Mol. Phys.* **1971**, *20*, 513.
(40) Rodriguez, J.; Kirmaier, C.; Holten, D. *J. Am. Chem. Soc.* **1989**, *111*, 6500.
(41) Baskin, J. S.; Yu, H. Z.; Zewail, A. H. *J. Phys. Chem. A* **2002**, *106*, 9837.
(42) Albota, M.; Beljonne, D.; Bredas, J.-L.; Ehrlich, J. E.; Fu, J.-Y.; Heikal, A. A.; Hess, S. E.; Kogej, T.; Levin, M. D.; Marder, S. R.; McCord-Maughon, D.; Perry, J. W.; Roumlckel, H.; Rumi, M.; Subramaniam, G.; Webb, W. W.; Wu, X.-L.; Xu, C. *Science* **1998**, *281*, 1653.
(43) Rumi, M.; Ehrlich, J. E.; Heikal, A. A.; Perry, J. W.; Barlow, S.; Hu, Z. Y.; McCord-Maughon, D.; Parker, T. C.; Rockel, H.; Thayumanavan, S.; Marder, S. R.; Beljonne, D.; Bredas, J. L. *J. Am. Chem. Soc.* **2000**, *122*, 9500.
(44) Dirk, C. W.; Herndon, W. C.; Cervanteslee, F.; Selnau, H.; Martinez, S.; Kalamegham, P.; Tan, A.; Campos, G.; Velez, M.; Zyss, J.; Ledoux, I.; Cheng, L. T. *J. Am. Chem. Soc.* **1995**, *117*, 2214.
(45) Cha, M.; Torruellas, W. E.; Yuan, S. H.; Stegeman, G. I.; Leclerc, M. *J. Opt. Soc. Am. B-Opt. Phys.* **1995**, *12*, 882.